

## Multiscale modeling investigation into the thermal conductivity dynamics of graphene-silver nano-composites: a molecular dynamic study

Q. Anjum<sup>a</sup>, N. Nasir<sup>b,\*</sup>, S. A. Cheema<sup>b</sup>, M. Imran<sup>a</sup>, A. R. Rahman<sup>c</sup>, Z. Tanveer<sup>a</sup>, N. Amin<sup>a</sup>, Y.N Anjam

<sup>a</sup>Physics Department, Government University Faisalabad, Pakistan

<sup>b</sup>Department of Applied Sciences, National Textile University Faisalabad, Pakistan

<sup>c</sup>Department of Statistics, Quaid-e-Azam University Islamabad, Pakistan

This research primarily aims at the in-depth exploration of thermal conductivity dynamics of Graphene-Silver (C-Ag) nano-composites on various parametric fronts. The parametric settings and resultant experimental states are mimicked by the rigorous launch of molecular dynamic (MD) simulations with Green-Kubo multiscale modeling approach. The enumeration of thermal conductivity of C-Ag nano-composites is instigated along with three orientations that is C-Ag (1 0 0), C-Ag (1 1 0) and C-Ag (1 1 1). Further, the conductive subtleties are expounded with respect to numerous factors of practical concerns such as, temperature, length of composite, composite width and number of Ag layers.

(Received December 9, 2021; Accepted April 29, 2022)

**Keywords:** Graphene-Silver nano-composite, Thermal conductivity, Equilibrium molecular dynamics simulations, Green-Kubo method

### 1. Introduction

This era of rapid technological growth is witnessing explosion of research targeting the fabrication of novel composites delivering extravagant structures projecting promising thermal conductivity. The issue of improved thermal conductivity has found serious implications in numerous professional and commercial applications associated with energy management, materialization of nano-devices, smart and complex system designs and electro-magnetic shielding [1-4]. Due to unique elegancies such as large surface area (2630 m<sup>2</sup>) [5], high thermal conductivity (~ 5000 Wm<sup>-1</sup>K<sup>-1</sup>) [6] and impressive mechanical strength (modules ~ 1.1 TPa) [7], the novel Graphene (C) has attained inspirational status of convincing nano-filler amongst available fillers for nano-composites reinforcement. As a result, metal-based C-metals composite structures are gaining overwhelmingly promising candidature in thermal conductivity driven usages [8, 9]. The C-metals compositions have been topic of various ongoing scientific research efforts. For example, [10] provided a comprehensive account of thermal characters of Graphene and its derivatives with respect to the applications in thermal interface materials. Similarly, [11-13] explored that the improved thermal conductivity and mechanical strength exhibited through C-metals composites generally depend on position along with arrangement of Graphene as well as metals. Moreover, [14] observed that C-metals nano-composites interface significantly affects thermal conductivity due to strong open *d-orbital* couplings. Furthermore, [15] focused on exploring the mechanical properties of C-metals interface in relation with dislocation gliding. For more interesting details, one may consult [16-18] comprehending the capability of Graphene's reinforcements and its derivatives to pin and annihilate dislocations. The impressive characters of C-metals nano-composites have earned prime candidature in wide range of multi-disciplinary usages such as, preparation of flexible wearable protective gears [19], production of automotive [20], health surveillance [21], intelligent systems development [22] and military applications [23].

Obliging the unique attributes of the C-metals, this article primarily aims at the exploration of thermal conductivity performance of C-Ag nano-composites. The inherent attributes

---

\* Corresponding author: nadeemnasir@ntu.edu.pk  
<https://doi.org/10.15251/DJNB.2022.172.557>

of Ag such as notable electric and thermal conductivity, superior mechanical strength, suitable optical reflectivity, flexibility and malleable transition-ability [24, 25], are also well documented. This research provides rich insight into the thermal dynamics of the C-Ag nano-composites by considering vibrant and diverse parametric settings. We considered three orientations of the C-Ag substrates such as, (1 0 0), (1 1 0) and (1 1 1). The thermal conductivities of these elaborative structures are then studied with respect to rich parametric settings considering varying levels of temperature, different levels of lengths of substrates, diverse settings incorporating width of composites and range of numbers of layers of Ag metal. The experimental environment is mimicked through rigorous application of molecular dynamic (MD) simulations with Green-Kubo multiscale modeling approach. Although, the experimental strategies constitute the premium tool to gather information regarding the material outlook, however, experimental enumeration of multi-dimensional complex states pose unanticipated challenges [26]. The launch of computational simulations of composites imitating the experimental environment to handle the above documented complexity remains well appreciated and reliable venue [27, 28]. The pictorial displays of simulated atomic configurations of structures under investigations are materialized with the application of visual molecular dynamics (VMD) procedure [29].

This article is divided into four major synchronized parts. The section 2 documents the details of simulation procedures employed to facilitate the goals of the research. Section 3 comprehends comprehensive discussions of the outcomes of the rigorously supported by relevant data and graphical displays. Lastly, section 4 summarizes the overall discussion of this investigation along with some future research possibilities.

## 2. Methods and Materials – Simulating Procedures

### 2.1. Model

The embedded behavior of C-Ag nano-composites is studied through the application of EM simulations by the adaptation of the soft of LAAMPS.

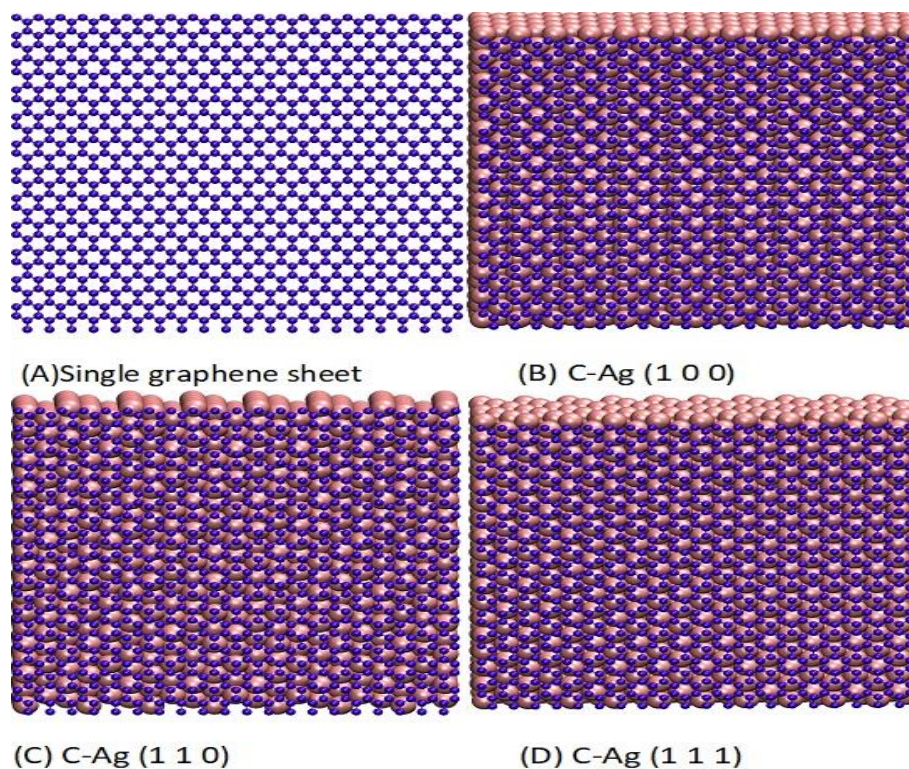


Fig. 1. Constructed molecular dynamics model for describing interactions in C-Ag system.

A stable configuration of hexagonal one atom thick C layer is stacked over the Ag substrate. Further, the study of thermal conductivity is proceeded along with three different orientations of the composite that is C-Ag (1 0 0), C-Ag (1 1 0) and C-Ag (1 1 1) with unit cell dimensions (50Å, 50Å, 50Å) for a time step of 0.182 fs. Moreover, the fixed wall effect is avoided by employing the periodic boundary conditions [30]. The steady-state is obtained with the assistance of Noose Hoover thermostat ensuring no time fluctuations while averaging the temperature. The visualization of the atomic structures of resultant structures is materialized through the visual molecular dynamics (VMD) program. After stabilizing the whole system, the canonical (NVT) ensemble is changed to a micro canonical (NVE) ensemble for better calculations [31, 32]. Then the thermal conductive characters of thus generated composite structures are explored with respect to temperature (300 K – 1000 K), length variations of 7.0 nm to 11.0 nm while keeping the temperature and width fixed, width levels of 0.8 nm to 2.0 nm over fixed length and temperature and varying number of layers of Ag from 1 layer to 5 layers. Figure 1 depict the simulated structure of the nano-composites in all pre-considered orientations along with a separate Graphene sheet.

## 2.2. Interatomic Potentials

We used Embedded Atom Method (EAM) potential [33] to describe interatomic interactions of Ag-Ag, whereas, generation Reactive Empirical Bond Order (REBO) potential [34] are used for the elaboration of C-C interactions. Moreover, the force between C-AG is enumerated through Lennard-Jones (LJ) potential [35]. The total energy of the system is written as;

$$E_{\text{Total}} = E_{\text{Ag}}^{\text{EAM}} + E_{\text{C}}^{\text{REBO}} + E_{\text{C-Ag}}^{\text{LJ}}. \quad (1)$$

The EAM can be written as a function of pair-wise interatomic interactions and embedding energy, such as;

$$E^{\text{EAM}} = \sum_i \left[ \frac{1}{2} \sum_{j \neq i} \Phi(r_{ij}) + F(\bar{\rho}_i) \right]. \quad (2)$$

Here,  $\bar{\rho}_i = \sum_{j \neq i} \rho(r_{ij})$  and represents the density through atomic density function  $\rho$ , where  $F$  is the associated embedding energy. Further,  $\Phi$  denotes pair potential triggered with the atom separation,  $r_{ij}$ . The REBO potential is given as;

$$E^{\text{REBO}} = \sum_i \sum_{j > i} [V_R(r_{ij}) - B_{ij}^* V_A(r_{ij})], \quad (3)$$

where,  $B_{ij}^*$  is bond-order parameter and  $V_R(r_{ij})$  represents the interatomic repulsion parameter with  $V_A(r_{ij})$  as interatomic attraction parameter. Lastly, the LJ potential modeling the interactions of C-Ag is given as;

$$E^{\text{LJ}} = 4\varepsilon \left[ \left( \frac{r_{ij}}{\sigma} \right)^{-12} - \left( \frac{r_{ij}}{\sigma} \right)^{-6} \right], \quad (4)$$

where, the parameters  $\varepsilon$  and  $\sigma$  describe the energy scale and collision diameter, respectively and are taken as  $\varepsilon_{\text{C-Ag}} = 0.0301 \text{ eV}$  and  $\sigma_{\text{C-Ag}} = 3.006 \text{ \AA}$  [36].

## 2.3. Green-Kubo Method

It is observed that the system remains constantly within the linear response regime during EMD simulation, therefore transport coefficients stay calculable through the Green-Kubo method. Thermal conductivity is interrelated throughout equilibrium current-current autocorrelation function using Green-Kubo expression is given as:

$$K = \frac{V}{k_B} T^2 \int_0^t J(t) J(0) > dt. \quad (5)$$

where,  $T$  is the system temperature,  $K_B$  is used to represent the Boltzmann's constant while  $t = m\sqrt{T}$  documents the support of correlation time in  $\sqrt{T}$  time steps of MD simulation along with  $V$  the volume of system equal to the product of area and Vander walls thickness ( $3.4\text{\AA}$ ). Meanwhile,  $J(t)J(0)$  is used for the denotation of heat current autocorrelation function (HCACF) which can be computed as:

$$J = \frac{1}{V} \sum_i e_i V_i - \sum_i S_i V_i. \quad (6)$$

Here,  $e_i V_i$  is total kinetic and potential energy and  $S_i V_i$  is stress tensor. The Green-Kubo method assists the accurate convergence of HCACF.

#### 2.4. Heat Transformation Mechanism in C-Ag Nano-composites

Thermal conductivity in C-Ag nano-composites delineates the transport of acoustic phonons in C and electrons in Ag by encompassing the relation of a temperature gradient with heat flux through Fourier's law. The relation is given such as  $J = -K\nabla T$ , where  $J$  is heat flux,  $K$  represents the thermal conductivity along temperature gradient  $\nabla T$ . The phonons and electron dependency of thermal conductivity in C and Ag, respectively is given as:

$$K = K_p + K_e, \quad (7)$$

where  $K_p$  is used for phonons and  $K_e$  stands for the electrons of Ag. Due to varying dominances of C and Ag, thermal conductivity drastically changes owing to modifications of phonons energies collectively with phonon scattering and phonons electrons scatterings. The acoustic phonon interactions through electrons in Ag reduced thermal conductivity appropriate to spatial confinement. Thermal conductivity, moreover, depends on size which changes phonons electrons interactions at the time of system alteration from 2D to 3D [37, 38]. Hence phonons boundary scatterings within C extensively affect thermal conductivity.

### 3. Results and Discussions

#### 3.1. Thermal Conductivity as a Function of Temperature

First, we assess the effect of temperature on the thermal conductivity of C-Ag nano-composites along all pre-defined orientations that is C-Ag (1 0 0), C-Ag (1 1 0) and C-Ag (1 1 1). A wide range of levels of temperature ranging from 300 K – 1000 K are considered to elaborate thermal conductivity of C-Ag composites as a function of temperature to facilitate the understanding of the phonons- phonons and phonons- electrons interactions in C-Ag system. The goals of the investigation are attained by simulating square sheet of Graphene of ( $50\text{\AA}$ ,  $50\text{\AA}$ ) with REBO potential. Table 1 comprehends the numerical outcomes highlighting the temperature effectiveness over the thermal conductivity of C-Ag nano-composites. Whereas, figure 2 depicts the underlying trends defining the functional linkages prevalent in the pre-set levels of temperature and resultant thermal conductivity of C-Ag nano-composites. One may immediately notice that the thermal conductivity along all orientations is inversely related to the varying levels of temperature through non-linear functional form. Moreover, the C-Ag (1 0 0) stands out as compared to contemporary structures with highest average extent of conductivity of  $445 \text{ Wm}^{-1}\text{K}^{-1}$  over the considered range of temperature that is 300 K – 1000 K. This is followed by orientation of C-Ag (1 1 0) with average offered conductivity of  $354.2 \text{ Wm}^{-1}\text{K}^{-1}$  which is almost of 20% lesser degree than leading C-Ag (1 0 0) orientation. Lastly, we estimated the performance of the C-Ag (1 1 1) structure with average thermal conductivity of  $298.6 \text{ Wm}^{-1}\text{K}^{-1}$  showing decrease of around 33% in comparison to the premium orientation of C-Ag (1 0 0).

Heat transfer in C is executed by acoustic phonons, while in Ag, it is transferred by electrons and thereby the interactions of phonons and electrons with the rise of temperature considerably affect thermal conductivity. Moreover, in disordered systems like composites, high-frequency phonons increase along with phonons umklapp scattering as a result of rising

temperature leading in the decay of thermal conductivity. Besides that, the interaction of acoustic phonons with optical phonons at higher temperature significantly affects the thermal conductivity of Graphene-metals composites [39]. Also, thermal conductivity remains explainable through mean free path indicating that heat transportation inside C-Ag system is not entirely diffusible and hence sharp temperature gradient possibly changes thermal conductivity. The number of short-wavelength phonons increases by increasing temperature.

Table 1. Thermal conductivity along with all orientation and varying levels of temperature.

Temperature (K)	C-Ag (1 0 0) ( $Wm^{-1}K^{-1}$ )	C-Ag (1 1 0) ( $Wm^{-1}K^{-1}$ )	C-Ag (1 1 1) ( $Wm^{-1}K^{-1}$ )
300 K	1210	1105	897
400 K	741	620	520
500 K	495	341	310
600 K	380	239	217
700 K	284	196	170
800 K	215	150	130
900 K	140	110	95
1000 K	95	73	50
Average Conductivity	445	354.2	296.8
% age Change w.r.t. prime orientation	---	20%↓	33%↓

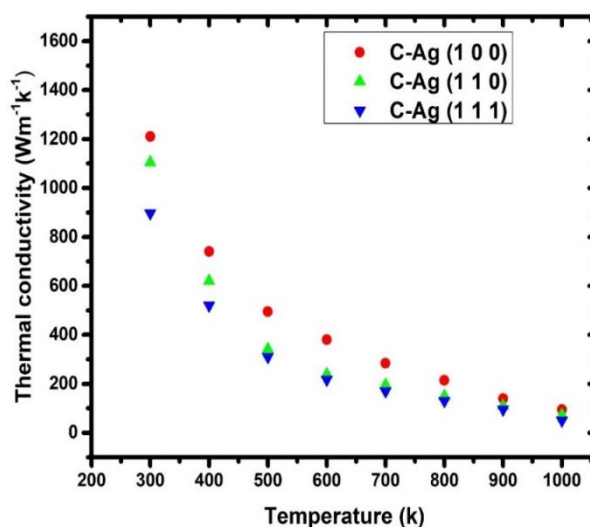


Fig. 2. Display of the thermal conductivity of C-Ag nano-composites along with all considered orientations over the pre-defined range of temperature.

### 3.2. Thermal Conductivity as a Function of Length of the Composite

The study of thermal conductivity of C-Ag nano-composites across all orientations is further proceeded with respect to the length of composites ranging from 7 nm to 11 nm. The linear extrapolation procedure is used to investigate thermal conductivity predictions for varying levels of length. Figure 3 provides the schematics of simulated structures over the considered range of length of composites. Few realizations are noticeable from Table 2 comprehending the numerical findings delineating the thermal conductivity of all pre-fixed orientations of C-Ag nano-composite. The C-Ag (1 1 0) orientation dominates the conductivity phenomenon across varying levels of lengths with an average value of  $2233 Wm^{-1}K^{-1}$ . The conductivity of this substrate is followed by C-Ag (1 0 0) orientation with associated average value of  $1908.2 Wm^{-1}K^{-1}$ , which shows an overall decrease of 14.5% as compared to the dominant (1 1 0) orientation. Lastly, we estimated thermal

dynamics of C-Ag (1 1 1) structure with offered average conductivity of  $1685 \text{ Wm}^{-1}\text{K}^{-1}$  inflicting overall decrement of 24.5% in comparison to the premium structure. Figure 4 depicts the functional relationship existent between length of the structures and perceived conductivity across all orientations. One may notice that the thermal conductivity is deemed to increase with increase lengths through non-linear fashion. This is witnessed with respect to all orientations.

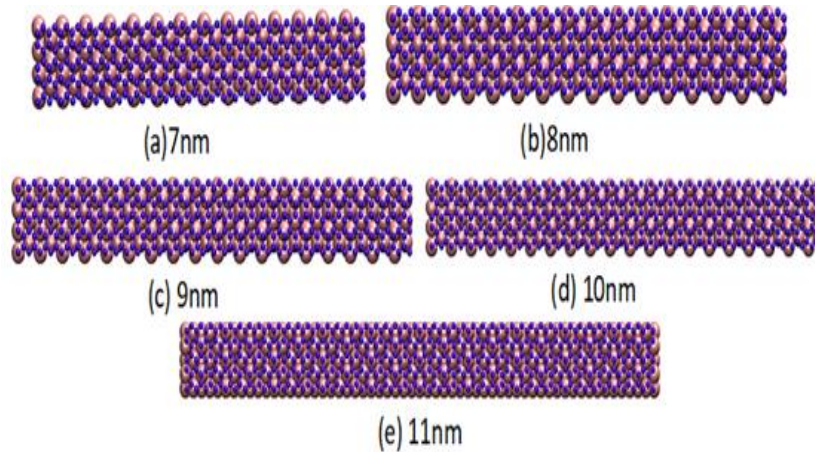


Fig. 3. Schematics of the simulated atomic structures of C-Ag nano-composites along with different levels of length.

It is noteworthy that flexural phonons play important role in the thermal conductivity behavior of Graphene when changes in length are induced whereas out-of-plane acoustic phonons are not known for the involvement in heat transportation [40]. Thus in this context, it is safe to anticipate that thermal conductivity dependence on length is mainly due to the phonons boundary scattering process. The variation in the length of composite dictate phonons mean free path and thereby the acoustic phonons of longer wavelength remain available in favor of larger length causing heavier heat transfer through the composite. As a result, phonons collision becomes defining phenomenon governing the scattering process and the Umklapp processes become negligible. The realizations of the on-going investigation verify the theoretical framework encompassing the relationship lying between thermal conductivity and length of composites.

Table 2. Thermal conductivity of C-Ag nano-composites with respect to varying levels of length across all orientations.

Length (nm)	C-Ag (1 0 0) ( $\text{Wm}^{-1}\text{K}^{-1}$ )	C-Ag (1 1 0) ( $\text{Wm}^{-1}\text{K}^{-1}$ )	C-Ag (1 1 1) ( $\text{Wm}^{-1}\text{K}^{-1}$ )
7	1218	1470	1034
8	1493	1796	1250
9	1785	2137	1526
10	2070	2512	1850
11	2975	3250	2765
Average Conductivity	1908.2	2233	1685
% age Change w.r.t. prime orientation	14.5%↓	---	24.5%↓

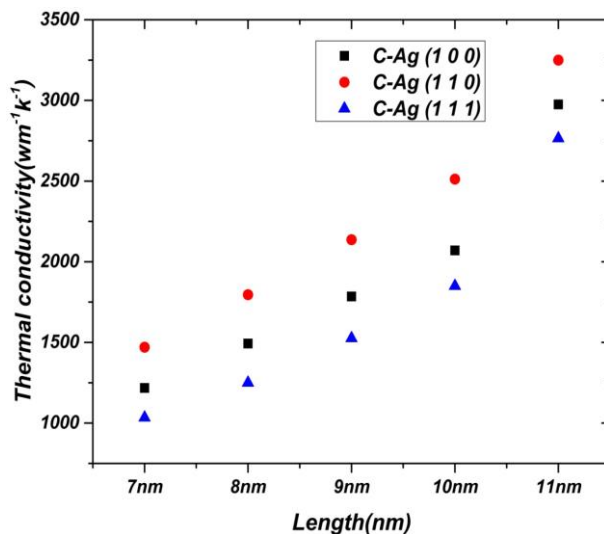


Fig. 4. Depiction of functional form exhibiting the relationship between levels of length and thermal conductivity of C-Ag nano-composites across all orientations.

### 3.3. Thermal Conductivity as a Function of Width

Now, we read the relational dynamics existent in the offered thermal conductivity of C-Ag nano-composites with respect to various levels of width of structures ranging from 0.80 nm to 2 nm with a jump of 0.2 nm. Figure 5 presents the schematics of atomic configuration of composites across varying levels of width. Whereas, Table 3 comprehends the numerical enumerations of projected thermal conductivity while relational dynamics are offered in figure 6. It can be seen that there exists non-linear increasing functional form deriving the relationship observant in the varying width levels and predicted thermal conductivity. The thermal conductivity increased with increase in width and these realizations are consistent across all pre-defined three orientations of the composites. Moreover, the C-Ag (1 1 0) orientation dominates the thermal conductivity application with average value of  $2748.8 \text{ Wm}^{-1}\text{K}^{-1}$ . The extent of thermal conductivity is then followed by C-Ag (1 0 1) orientation with associated average value of  $2103.4 \text{ Wm}^{-1}\text{K}^{-1}$ , which is of around 23.5% lesser degree than the dominant structure. Lastly, we observed C-AG (1 1 1) orientation with average thermal conductivity over the range of width of  $1796.6 \text{ Wm}^{-1}\text{K}^{-1}$  revealing decrease of 34.6% as compared to (1 0 0) orientation.

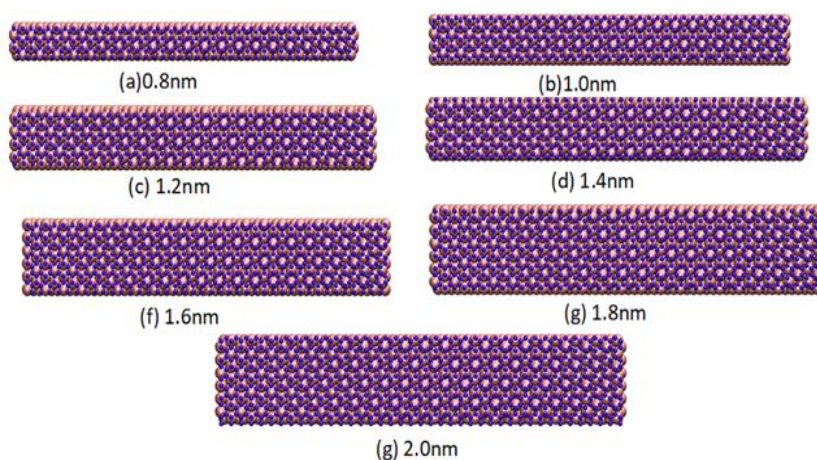


Fig. 5. Schematics of the simulated atomic structures of C-Ag nano-composites along with different levels of width.

Table 3. Thermal conductivity of C-Ag nano-composites with respect to varying levels of width across all orientations.

Width (nm)	C-Ag (1 0 0) ( $Wm^{-1}K^{-1}$ )	C-Ag (1 1 0) ( $Wm^{-1}K^{-1}$ )	C-Ag (1 1 1) ( $Wm^{-1}K^{-1}$ )
0.8	972	1233	760
1.0	1334	1543	1011
1.2	1573	2043	1352
1.4	1969	2649	1680
1.6	2336	3299	1991
1.8	2936	3932	2565
2.0	3604	4543	3217
Average Conductivity	2103.4	2748.8	1796.6
% age Change w.r.t. prime orientation	23.5%↓	---	34.6%↓

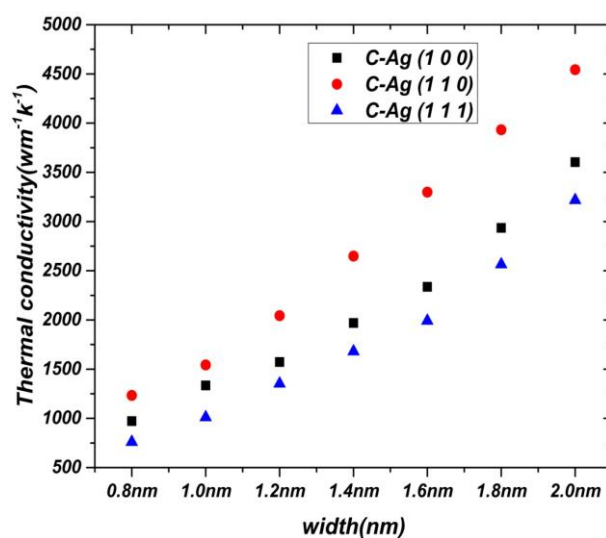


Fig. 6. Depiction of functional form exhibiting the relationship between levels of width and thermal conductivity of C-Ag nano-composites across all orientations.

It is documented that the effect of electrons in the metal, the edge localized phonons, phonons umklapp, along with boundary scattering in C drastically change composite thermal conductivity [41]. In favor of increase in width, thermal conductivity monotonically increases with increase in width due to boundary scattering along with Umklapp scattering. Also, by increasing width, reduction in edge localized phonon also occurs and therefore boundary scattering increases in C which in turn increases the number of phonons. Thus the electron and phonons interactions in C-Ag nano-composites significantly improves thermal conductivity by increasing width.

### 3.4. Thermal Conductivity as a Function of Silver Substrate

Lastly, we elaborate the effect of number layers of Ag substrate on the thermal conductivity of C-Ag nano-composite. We consider variation in Ag layers ranging from one layer to five layers. Figure 7 presents the schematics of the simulated atomic configuration of nano-structures along with all considered number of layers.

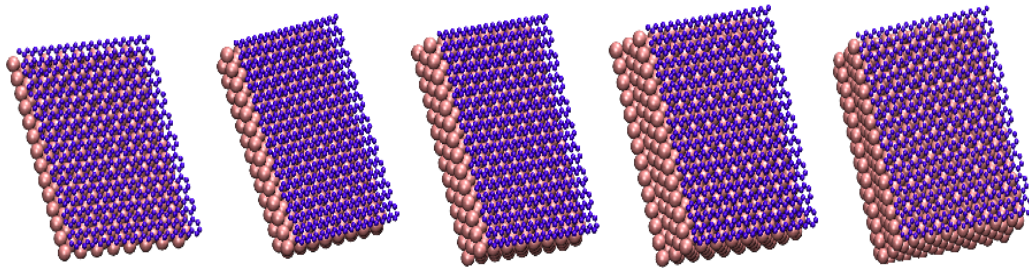


Fig. 7. Schematics of atomic structures of C-Ag nano-composites with respect to number of layers varying from single layer (left panel) to five layers (right panel).

Table 4 presents the predicted intensity of thermal conductivity of C-Ag nano-composites with respect to all variations of layer and across all orientations. Also, the functional form depicting the nature of relationship lying between layer variations and offered thermal conductivity is documented in Figure 8. One may notice the existence of decreasing relationship linking number of layers and thermal conductivity through a slight non-linear form. That is, the thermal conductivity is deemed to decrease as the number of layers of Ag increases. Moreover, we observed that C-Ag (1 0 0) orientation dominates the thermal conductivity with average value of  $1237.6 \text{ Wm}^{-1}\text{K}^{-1}$ . This premium orientation is followed by C-Ag (1 1 0) with associated value of  $1092.2 \text{ Wm}^{-1}\text{K}^{-1}$  which indicates decrease of 11.7% as compared to the dominant orientation. Lastly, we estimate C-Ag (1 1 1) orientation with average value of  $908.6 \text{ Wm}^{-1}\text{K}^{-1}$  projecting decrease of 26.6% in comparison to the prime (1 0 0) orientation.

Table 4. Thermal conductivity of C-Ag nano-composites with respect to varying number of layers across all orientations.

Number of silver layers	C-Ag (1 0 0) ( $\text{Wm}^{-1}\text{K}^{-1}$ )	C-Ag (1 1 0) ( $\text{Wm}^{-1}\text{K}^{-1}$ )	C-Ag (1 1 1) ( $\text{Wm}^{-1}\text{K}^{-1}$ )
1	2037	1892	1507
2	1406	1259	1063
3	1148	993	872
4	909	742	650
5	688	575	451
Average Conductivity	1237.6	1092.2	908.6
% age Change w.r.t. prime orientation	---	11.7%↓	26.6%↓

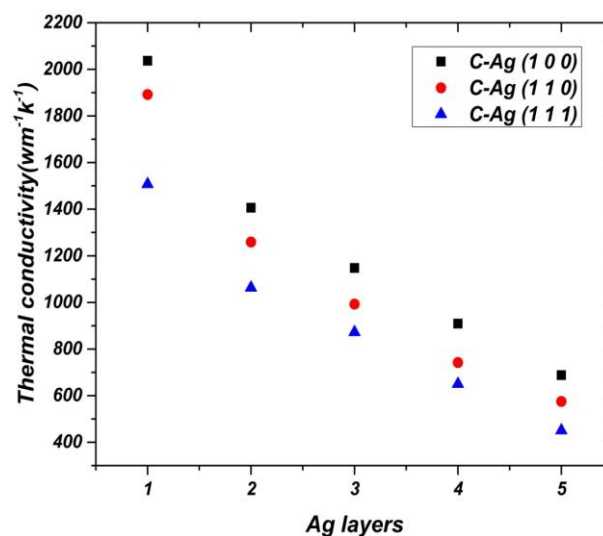


Fig. 8. Depiction of functional form exhibiting the relationship between varying number of layers and thermal conductivity of C-Ag nano-composites across all orientations.

#### 4. Conclusions

This research mainly target the study of heat transport characteristics in Graphene-silver nano-composites along three orientations such as C-Ag (1 0 0), C-Ag (1 1 0) and C-Ag (1 1 1), with respect to various factors anticipated as influencer in thermal conductivity phenomenon. Silver (Ag) is amongst the highly regarded materials with wide applicability in numerous commercial and professional usages, however, it offers lower thermal conductivity. Thereby, academic circles involved in conductive materials research remain eager to pursue novel procedures adding towards the improved thermal attributes of the Ag substrates. Motivated by the excellent thermal behaviors of profound honey-comb structure of Graphene (C), this research elaborates the conductive norms of C-Ag nano-composites with respect to various interlinked parameterizations.

We considered range of temperature, various levels of length of composites, different levels of width and variations of number of layers of Ag substrate. The experimental states are mimicked through the application of EMD simulations by the Green Kubo method. Moreover, visualization of the atomic configurations of composites are materialized through Visual Molecular Dynamics (VMD). We observed that the thermal conductivity of the nano-composite remains orientation sensitive. The temperature is found to be negatively associated with thermal conductivity – thermal conductivity is deemed to be decreasing with increase in temperature. We estimated the performance ordering such as,  $C - Ag(1\ 0\ 0) > C - Ag(1\ 1\ 0) > C - Ag(1\ 1\ 1)$ . Further, we observed increased thermal conductivity in case of increased length of composites with underlying performance hierarchy  $C - Ag(1\ 1\ 0) > C - Ag(1\ 0\ 0) > C - Ag(1\ 1\ 1)$ . In case of the effectiveness of width, we found positive association between varying levels of width and predicted thermal conductivity. The ranking of nano-composites is quantified as  $C - Ag(1\ 1\ 0) > C - Ag(1\ 0\ 0) > C - Ag(1\ 1\ 1)$ . Lastly, number of layers of Ag substrate are seen to defining thermal conductivity in decreasing manner with performance prominence of  $C - Ag(1\ 0\ 0) > C - Ag(1\ 1\ 0) > C - Ag(1\ 1\ 1)$ .

These results provide encouraging insight into the interlinks existent in Graphene-Metals composite materials. The applications remain intact along various multi-disciplinary fronts engaged in energy management, facilitation of the problem of heat dissipation.

#### Reference

- [1] Santhosi, B. V. S. R. N., Ramji, K. and Rao, N. M. *Physica B: Condensed Matter*, 586, 412144(2020); <https://doi.org/10.1016/j.physb.2020.412144>
- [2] Tuček, J., Błoński, P., Ugolotti, J., Swain, A. K., Enoki, T. and Zbořil, R. *Chemical Society Reviews*, 47 (11), (2018); <https://doi.org/10.1039/C7CS00288B>
- [3] Parfen'eva, L. S., Orlova, T. S., Smirnov, B. I., Smirnov, I. A., Misiorek, H., Jezowski, A. and Ramirez-Rico, J. *Physics of the Solid State*, 56 (5), (2014).
- [4] Xu, Z. and Buehler, M. J. *Journal of Physics: Condensed Matter*, 22 (48), 485301(2010); <https://doi.org/10.1088/0953-8984/22/48/485301>
- [5] Nesov, S. N., Bolotov, V. V., Korusenko, P. M., Povoroznyuk, S. N. and Vilkov, O. Y. *Physics of the Solid State*, 58 (5), (2016); <https://doi.org/10.1134/S1063783416050164>
- [6] Galashev, A. E. E. and Rakhmanova, O. R. *Physics-Uspekhi*, 57 (10), (2014); <https://doi.org/10.3367/UFNe.0184.201410c.1045>
- [7] Ferrari, A. C., Bonaccorso, F., Fal'Ko, V., Novoselov, K. S., Roche, S., Bøggild, P. and Garrido, J. *Nanoscale*, 7 (11), (2015).
- [8] Zhang, L., Zhu, W., Huang, Y. and Qi, S. *Nanomaterials*, 9 (9), (2019); <https://doi.org/10.3390/nano9091264>
- [9] Huang, J., Yang, W., Zhu, J., Fu, L., Li, D. and Zhou, L. *Composites Part A: Applied Science and Manufacturing*, 123, (2019); <https://doi.org/10.1016/j.compositesa.2019.05.002>
- [10] Shahil, K. M. and Balandin, A. A. *Solid State Communications*, 152 (15), (2012);

<https://doi.org/10.1016/j.ssc.2012.04.034>

- [11] Han, R. Q., Song, H. Y., Wang, J. Y. and Li, Y. L. *Physica B: Condensed Matter*, 601, (2021); <https://doi.org/10.1016/j.physb.2020.412620>
- [12] Sharma. S., Kumar, P. and Chandra, R. *Journal of Composite Materials*, 51 (23), (2017); <https://doi.org/10.1177/0021998316682363>
- [13] Khan. M., Tahir, M. N., Adil, S. F., Khan, H. U., Siddiqui, M. R. H., Al-warthan, A. A. and Tremel, W. *Journal of Materials Chemistry A*, 3 (37), (2015); <https://doi.org/10.1039/C5TA02240A>
- [14] Kandare. E., Khatibi, A. A., Yoo, S., Wang, R., Ma, J., Olivier, P. and Wang, C.H. *Composites Part A: Applied Science and Manufacturing*, 69, (2015); <https://doi.org/10.1016/j.compositesa.2014.10.024>
- [15] Charlestona J., Agrawala, A. and Mirzaeifar R. *Comput. Mat. Sci.*, 0927-0256 (2020).
- [16] Agrawal, A. and Mirzaeifar, R. *Surface Sci.*, 688, (2019); <https://doi.org/10.1016/j.susc.2019.05.003>
- [17] Kalcher C., Brink, T., Rohrer, J., Stukowski, A. and Albe, K. *Phys. Rev. Mater.*, 3 (9), (2019); <https://doi.org/10.1103/PhysRevMaterials.3.093605>
- [18] Duan K., Zhu F., Tang K., He L., Chen Y. and Liu S. *Comput. Mat. Sci.*, 117, (2016); <https://doi.org/10.1016/j.commatsci.2016.02.007>
- [19] Shathi M. A., Chen M., Khoso N. A., Rahman Md. T. and Bhattacharjee B. *Materials and Design*. 193, (2020); <https://doi.org/10.1016/j.matdes.2020.108792>
- [20] Elmarakbi A. and Azoti W. *Micro and Nano Technologies*. 1-23 (2018); <https://doi.org/10.1016/B978-0-323-48061-1.00001-4>
- [21] Huang H., Su S., Wu N., Wan H., Wan S., Bi H. and Sun L. *Front. Chem.* 7 (399), (2019); <https://doi.org/10.3389/fchem.2019.00399>
- [22] Zang Y., Zhang F., Di C. A. and Zhu D. *Mater. Horiz.* 2, (2015); <https://doi.org/10.1039/C4MH00147H>
- [23] Joshi S., Kumar A. and Zaidi M. *Def. Sci. J.* 70 (3), (2020); <https://doi.org/10.14429/dsj.70.15357>
- [24] Zhang X., Liu Z., Shen W. and Gurunathan S. *Int. J. Mol. Sci.* 17 (1534), (2016); <https://doi.org/10.3390/ijms17091534>
- [25] Orłowski P., Tomaszewska E., Gniadek M., Baska P., Nowakowska, J., et al. *PLoS ONE*. 9, (2014); <https://doi.org/10.1371/journal.pone.0104113>
- [26] Zhou X., Liu X., Lei J. and Yang Q. *Computational Materials Science*, 172, 109342, (2020); <https://doi.org/10.1016/j.commatsci.2019.109342>
- [27] Shariatinia Z. and Mazloom-Jalali A. *Chinese Journal of Physics*. 66, (2020); <https://doi.org/10.1016/j.cjph.2020.04.012>
- [28] Vatanparast M. and Shariatinia Z. *J. Mater. Chem. B*. 7, (2019); <https://doi.org/10.1039/C9TB00971J>
- [29] Jalali S. K., Beigrezaee M. J. and Pugno N. M. *Phys E Low Dimen Syst Nanostruct.* 93,(2017); <https://doi.org/10.1016/j.physe.2017.06.031>
- [30] Madec. R., Devincre, B. and Kubin, L. In *IUTAM Symposium on mesoscopic dynamics offracture process and materials strength* (pp. 35-44).Springer, Dordrecht (2004); [https://doi.org/10.1007/978-1-4020-2111-4\\_4](https://doi.org/10.1007/978-1-4020-2111-4_4)
- [31] Mori.Y. and Okamoto, Y. *Journal of the Physical Society of Japan*, 79 (7), (2010); <https://doi.org/10.1143/JPSJ.79.074003>
- [32] Kraska. T. *The Journal of chemical physics*, 124 (5), (2006); <https://doi.org/10.1063/1.2162882>
- [33] Zhou, X., Liu X., Lei J. and Yang Q. *Computational Materials Science*. 109342, (2019); <https://doi.org/10.1016/j.commatsci.2019.109342>
- [34] Dewapriya M. A. N., Rajapakse R. K. N. D. and Nigam N. *Carbon*. 93, (2015); <https://doi.org/10.1016/j.carbon.2015.05.101>

- [35] Sadeghzadeh S. J Mol Graph Model. 70, (2016); <https://doi.org/10.1016/j.jmgm.2016.10.001>
- [36] Lia L., Suna R., Zhanga Y., Kitipornchaic K. and Yang J. Computational Materials Science. 182, 109759 (2020); <https://doi.org/10.1016/j.commatsci.2020.109759>
- [37] Huang. J., Yang, W., Zhu, J., Fu, L., Li, D. and Zhou, L. Composites Part A: Applied Science and Manufacturing, 123, (2019); <https://doi.org/10.1016/j.compositesa.2019.05.002>
- [38] Kumar S. Mater Chem Phys. 202, (2017).
- [39] Nika. D. L., Ghosh, S., Pokatilov, E. P. and Balandin, A. A. Applied Physics Letters, 94 (20), (2009) <https://doi.org/10.1063/1.3136860>
- [40] Sonvane. Y., Gupta, S. K., Raval, P., Lukačević, I. and Thakor, P. B. Chemical Physics Letters, 634, (2015); <https://doi.org/10.1016/j.cplett.2015.05.036>
- [41] Evans. W. J., Hu, L. and Keblinski, P. Applied Physics Letters, 96 (20), (2010); <https://doi.org/10.1063/1.3435465>